Dielectric Properties of Yeast Cells Expressed With the Motor Protein Prestin

JOHN H. MILLER JR.^{1,*}, DHARMAKEERTHI NAWARATHNA¹, DAVID WARMFLASH¹, FRED A. PEREIRA^{2,3,4} and WILLIAM E. BROWNELL^{2,5}

¹Department of Physics and Texas Center for Superconductivity & Advanced Materials, University of Houston, 4800 Calhoun Road, Houston, Texas 77204-5005, U.S.A.; ²Department of Otorhinolaryngology, Baylor College of Medicine, One Baylor Plaza, Houston, Texas 77030, U.S.A.; ³Department of Molecular and Cellular Biology, Baylor College of Medicine, One Baylor Plaza, Houston, Texas 77030, U.S.A.; ⁴Huffington Center on Aging, Baylor College of Medicine, One Baylor Plaza, Houston, Texas 77030, U.S.A.; ⁵Department of Neuroscience, Baylor College of Medicine, One Baylor Plaza, Houston, Texas 77030, U.S.A. (*Author for correspondence, e-mail: jhmiller@uh.edu)

Abstract. We report on the linear and nonlinear dielectric properties of budding yeast (*S. cerevisiae*) cells, one strain of which has been genetically modified to express prestin. This motor protein plays a crucial role in the large electromotility exhibited by the outer hair cells of mammalian inner ears. Live cell suspensions exhibit enormous dielectric responses, which can be used to probe metabolic activity, membrane potential, and other properties. The aims of this study are: (1) to compare the dielectric responses of organisms expressing prestin from those of control specimens, and (2) ultimately to further develop dielectric response as a tool to study live cells, proteins, and lipids.

Key words: dielectric spectroscopy, cochlea, outer hair cells, motor proteins, prestin, budding yeast, *S. cerevisiae*

Introduction: Background and Motivation

Dielectric spectroscopy is a powerful method for noninvasively characterizing the properties of biological systems [1–12]. It encompasses the frequency dependence of the complex linear dielectric response, which incorporates both the dielectric constant $\varepsilon(\omega)$ and the conductivity $\sigma(\omega)$ of the medium. In addition, biological systems and complex macromolecules, such as proteins, exhibit pronounced *nonlinear* responses, which can be manifested in a number of ways, including the production of harmonics of the applied frequency or mixing responses at sum or difference frequencies between two applied frequencies.

Prestin is a recently discovered transmembrane protein found in the outer hair cells of the mammalian cochlea [13–21]. It is attracting increasing attention from cell biologists and biophysicists, because it contributes to a mechanism that

enhances the ability of membranes to directly convert voltage to force at microsecond rates, and is unlike conventional motor molecules based on enzymatic activity. Together with cytoplasmic anions, prestin enhances the electromotility of outer hair cells, and is believed to play a key role in hearing amplification at high frequencies in the mammalian inner ear.

BACKGROUND ON DIELECTRIC SPECTROSCOPY

Early work on dielectric spectroscopy of biological systems was carried out by Schwan [1], who characterized the dielectric properties of human tissue. His studies found that the low-frequency dielectric response of biological systems is enormous, but decreases rapidly with increasing frequency. More recently, Asami [2] and others [3] performed a variety of studies on live cell suspensions, including some on budding yeast (*S. cerevisiae*) that showed significant changes in dielectric response with time, reflecting cell respiration, metabolism, and reproduction. Prodan [4, 5] performed theoretical modeling studies, predicting a correlation between the low frequency dielectric constant and the magnitude of the cellular transmembrane potential. This is consistent with observations, since human erythrocytes (red blood cells), with small membrane potentials, have orders of magnitude lower dielectric constants at low frequencies than *S. pombe* (fission yeast) cells, which have much larger membrane potential magnitudes of about 200 mV.

Our group has developed several techniques for improving sensitivity and reducing electrode polarization effects. One method [6] employs high- T_c superconducting quantum interference devices (SQUIDs) to directly probe the tiny ac magnetic fields produced by the displacement currents. Another technique [7] uses conventional electronics, but uses a variable electrode spacing calibration technique to subtract the spurious low-frequency capacitance created by the dipole layers at the electrodes. Groundbreaking work on *nonlinear* response was spearheaded by Woodward and Kell [8, 9], who correlated the generation of harmonics with changes in the conformational states of membrane proteins.

Several distinct dispersions (or relaxations), notably α -, β -, and γ -dispersions, have been identified [1] in the linear dielectric spectra of biological cell suspensions and tissues over the frequency range 1 Hz–10 GHz. The α -dispersion, which appears below several kHz and is the subject of this study, results from several mechanisms, including the displacement of counter ions surrounding charged membranes, the polarization of intracellular charges, and the rotational orientation of large macromolecules with electric dipole moments. The β -dispersion, typically observed at MHz frequencies, is primarily attributed to the dielectric properties of the insulating membranes surrounding the cells and internal organelles. This is supported by the fact that the β -dispersion nearly disappears in cells whose membranes have been disrupted or permeabilized by detergents. The γ -dispersion, which results from re-orientation of water and other molecules, lies above 1 GHz. Between the β - and γ -dispersions, there are often numerous small dispersions, which show up as peaks

in the imaginary part of the dielectric response, due to the relaxation of biopolymers and bound water.

Remarkably, the charge density in the peripheral cytoskeleton of a yeast cell, which typically has a membrane potential of $-200 \, \mathrm{mV}$ relative to the extracellular medium, can exceed 10^{21} electrons/cm³. This is comparable to or higher than the carrier concentration of a high- T_c superconductor, and orders of magnitude higher than that of a doped semiconductor. This negative charge is partly due to anions (e.g. $\mathrm{Cl^-}$ ions) inside the cell, but perhaps an even greater contribution comes from negatively charged proteins and nucleic acids. For example, each of the numerous F-actin filaments, which comprise a major component of the cytoskeleton, has a linear charge density of $-1.7 \, \mathrm{e/\mathring{A}}$, while each DNA helix has a charge per unit length of $-2.5 \, \mathrm{e/\mathring{A}}$. However, unlike a semiconductor, metal, or superconductor, the motion of these cellular charges is constrained. Thus, at least the qualitative features of the low-frequency alpha-response of a live cell suspension can be modeled as the overdamped motion of a large number of charged particles, each sitting in its own harmonic restoring potential, in a viscous fluid.

If we treat a cell membrane of area A and thickness d as a capacitance $C_m = \varepsilon_m A/d$, where ε_m is the dielectric constant of the membrane, and approximate the cell interior as an equipotential, then the charge inside the cell is simply $Q = C_m V_m$, where V_m is the membrane potential. Treating each charge Q (of mass m) as a driven overdamped oscillator (of resonant frequency ω_0 in the absence of damping), the equation of motion in response to an electric field E(t) is given by $dx/dt + \omega_0^2 \tau' x(t) = (Q\tau'/m)E(t)$. For an applied field $E(t) = E(\omega)\exp[i\omega t]$ and response $x(t) = x(\omega)\exp[i\omega t]$, the solution is $x(\omega) = (Q\tau'/m)E/[i\omega + 1/\tau]$, where $\tau = 1/\omega_0^2 \tau'$ is known as the Debye relaxation time. The total current density is given by J(t) = nQ(dx/dt) so, in the frequency domain, $J(\omega) = i\omega nQx(\omega)$, where n is the concentration of cells per unit volume. This yields the result $J(\omega) = \{i\omega nV_m^2K[i\omega + 1/\tau]^{-1}\}E(\omega) = \sigma(\omega)E(\omega)$, where $K = C_m^2 \tau'/m$, and the term in brackets is the complex conductivity s(w) of the suspension. The complex dielectric constant is related to the conductivity by $\varepsilon^*(\omega) = \sigma(\omega)/i\omega$. When added to the high-frequency dielectric constant ε_∞ of the medium, this yields the result:

$$\varepsilon^* = \frac{\varepsilon_s - \varepsilon_\infty}{1 + i\omega\tau} + \varepsilon_\infty,\tag{1}$$

where τ is the Debye relaxation time and $\varepsilon_s - \varepsilon_\infty = nV_m^2 K$ is the limiting low-frequency contribution by the cell suspension. In the literature on dielectric spectroscopy, it is conventional to refer to the complex dielectric response as ε^* rather than ε . (Note that ε^* does *not* refer to the complex conjugate in this case.)

Real cells are, of course, vastly more complex than the simple picture above would suggest. Eukaryotes contain numerous internal organelles, some, such as the mitochondria, functioning nearly as independent organisms. In fact each mitochondrion has its own rather large membrane potential, with a magnitude of

about 250 mV. Even bacteria, which are prokaryotes, have a surprising internal complexity, although they lack many of the organelles (microtubules, endoplasmic reticulum, nucleus, etc.) of eukaryotes. Because of this complexity, the system is more appropriately modeled as having a broad distribution of relaxation times and other parameters. A type of relaxation observed in disordered materials, called the "universal dispersion pattern," was first reported by Jonscher [10], and exhibits a constant phase scaling law $e^* \sim (i\omega)^{n-1}$. Often the behavior is neither ideal Debyelike nor pure power law. For such combined responses, fractal models have been proposed [11, 12].

BACKGROUND ON PRESTIN, A MOTOR PROTEIN INVOLVED IN HEARING

The mammalian ear owes its amazing sensitivity, frequency range, and frequency resolving capability to amplification, with up to a thousand-fold gain, provided by the outer hair cells (OHCs) [13, 14] residing in the organ of Corti. This hearing sense organ, located in the cochlea, also contains the inner hair cells (IHCs), which function as the sensory receptors of sound and convey auditory information to the brain. The mechanical amplification mechanism of OHCs has been found to result from extraordinary levels of electromotility, orders of magnitude higher than that of any commercial piezoelectric crystal. Like all hair cells, OHCs have stereocilia bundles that, when deflected, trigger the opening and closing of mechanosensitive ion channels [15]. This causes, in turn, rapid changes in the trans-membrane potential of the OHC, which propagate down the length (up to 60 mm long) of its cylindrical body. However, unlike other hair cells, the OHC converts these voltage changes into macroscopic changes in its length. Depolarization triggers cell contraction, whereas hyperpolarization triggers cell elongation. This electrically driven cell motility responds to each sound cycle and generates mechanical energy that is transmitted into the tectorial and basilar membranes at the proper phase needed to amplify sound-induced vibrations in the cochlea. In the absence of the amplification provided by OHCs, hearing sensitivity is severely degraded and the ear's frequency-resolving capability is compromised.

The outer hair cell is a unique cylindrical structure that lacks an internal cytoskeleton and functions as a hydrostat. Its electromotility results from a membrane-based motor that resides in the cell's lateral wall, which is a composite structure with nanoscale dimensions. Three layers are found within 100 nm of the cell's surface [16], as shown in Figure 1: (1) the plasma membrane, (2) a highly organized cortical lattice made up of cytoskeletal proteins, including F-actin, spectrin, and a yet-to-be-identified, pillar-shaped protein, and (3) a novel subcellular organelle called the subsurface cisterna. This trilaminate organization is unique to the outer hair cell, as is its electromotility, which takes place without hydrolysis of energetic phosphates, such as ATP. Moreover, Ca²⁺ ions are not required for the expression of the OHC's electromotile response. Finally, this electromotile response occurs at microsecond rates and works in a cycle-by-cycle mode at frequencies approaching 100 kHz.

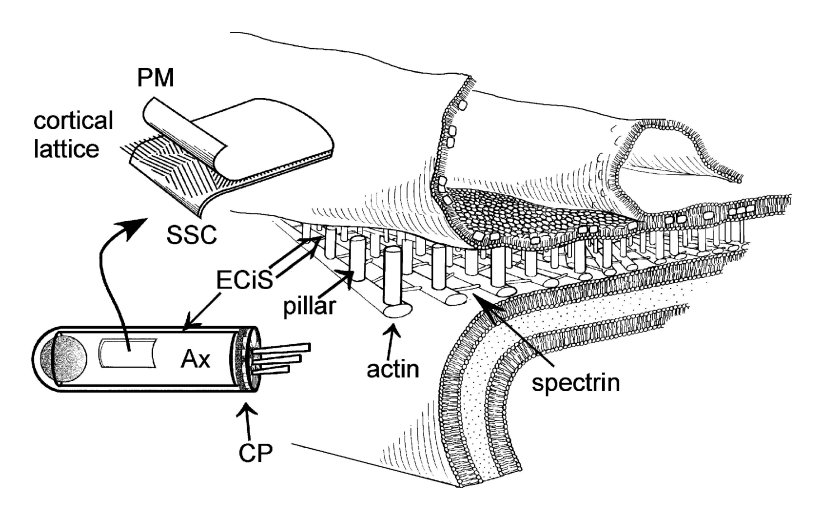


Figure 1. Diagram of OHC with detail of lateral wall components. Axial core (Ax), extracisternal space (ECiS), subsurface cisterna (SSC), cuticular plate (CP). The lateral wall consists of an outermost plasma membrane (PM), a cortical lattice and the SSC, all of which lie within 100 nm of the cell's surface and are concentrically organized about the cell's longitudinal axis.

In addition to the above features, a recently discovered motor protein in the outer membrane, known as prestin [17, 18], has been found to greatly enhance the OHC's electromotility. Prestin shows homologies to sulfate transporters, which are members of an ancient family of integral membrane proteins that facilitate anion transport across membranes. The protein contains twelve hydrophobic domains, which presumably pass through the membrane as either alpha helices or beta sheets and are linked by charged amino acid sequences that span the extracellular and cytoplasmic regions, perhaps like the folds of an accordion. The mechanism by which prestin operates is still poorly understood. One model [18], based on studies [19] showing the importance of anion concentration in the OHC cytoplasm, proposes that prestin operates as an incomplete anion (e.g. Cl⁻) transporter. According to this model, in the absence of internal Cl⁻, the OHC and prestin molecule are in their 'short' (depolarized) states. When enough internal Cl⁻ anions exist to drive the membrane potential into a hyperpolarized state, some of these anions are partially translocated through the membrane by the prestin molecule, thus driving (by an unknown mechanism) the prestin molecule, and thus the OHC, into their 'long' states.

The electromotility of OHCs has been found to show an almost perfect correlation with an observed nonlinear capacitance (NLC) [20, 21], which exhibits a bell-shaped curve when plotted as a function of membrane potential and adds to the intrinsic linear capacitance of the membrane. The shape of the NLC curve reflects the partial translocation of charges through the membrane, and peaks at the voltage that is most effective in producing a motile response of the OHC. Since nonlinear capacitance is straightforward to measure with good accuracy, it is often used as a

'signature' of electromotility rather than directly measuring changes in cell length. NLC has been found to be reversibly eliminated by removing Cl⁻ from the cytoplasm of cells containing prestin [19]. This supports the notion that monovalent anions partially translocating through the protein trigger conformational changes that alter its surface area in the plane of the plasma membrane. Moreover, the observed correlation between NLC and electromotility suggests that dielectric spectroscopy, which probes total capacitance versus frequency, may potentially be used as a noninvasive probe of cells that have been genetically modified to express prestin. Of particular interest, for example, is a comparison to recent observations [22] of frequency-dependent electrical resonances in OHCs, isolated from the apical turn of the cochlea, exhibiting features analogous to classical piezoelectric transducers.

Materials and Methods

In a project designed to carry out structure-function mutagenesis analysis of prestin, a bioinformatics approach, known as evolutionary trace analysis, is used to identify residues for targeted mutations, deletions, and fragment swaps. The results of functional assays will ultimately enable further refinement of computational experiments and permit modeling of prestin's tertiary structure and its mode of interaction within the outer hair cell membrane. For this study, two cultures of genetically modified yeast (*S. cerevisiae*) were grown. One strain was designed to express prestin when copper sulfate (CuSO₄) was added to the growth medium, as well as glutathione-s-transferase (GST), while the other expressed only GST as a control protein. The two cultures were resuspended in deionized water at a concentration of 10⁸ cells/ml, and linear dielectric response measurements were carried out, as discussed below, using the setup shown in Figure 2. In addition, nonlinear

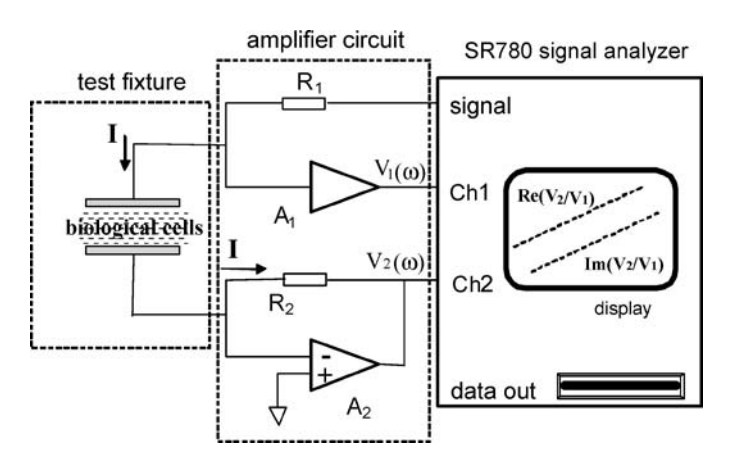


Figure 2. Setup, using a Stanford Research SR780, for measuring the complex linear dielectric response (real and imaginary parts) of a live cell suspension, in which the electrodes are in direct contact with the medium.

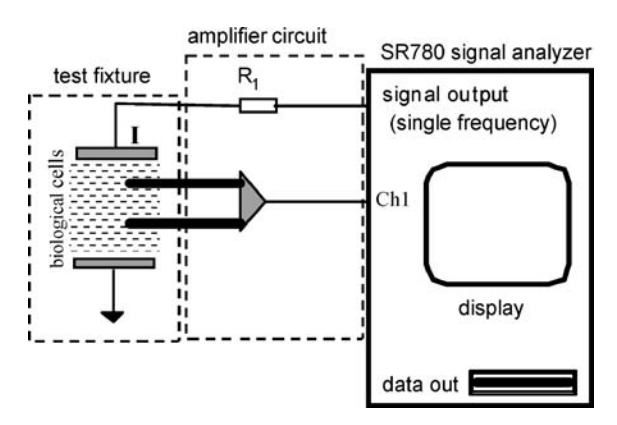


Figure 3. Setup used to measure the nonlinear harmonic response of a live cell suspension using a four-electrode technique.

properties, in which several harmonics were induced by the cell suspension in response to an applied fundamental frequency, were measured for the two strains, using the setup shown in Figure 3.

For linear dielectric response measurements, the reference voltage waveform from the signal analyzer in Figure 2 is applied to the upper electrode through resistor R_1 . The Stanford Research SR780 FFT Vector Signal Analyzer provides a swept frequency sinusoidal voltage at its reference output. It digitizes the inputs to Channels 1 and 2 in the time domain, takes the fast Fourier transform (FFT) to determine the relative magnitudes and phases of the input voltages $V_1(\omega)$ and $V_2(\omega)$ in the frequency domain, and also computes the complex ratio of these two amplitudes V_2/V_1 . The real and imaginary parts of V_2/V_1 versus frequency are then stored on a floppy disk for additional processing on a computer. The bottom electrode of the cell suspension capacitor is connected to the negative input of amplifier A_2 , which holds this electrode at ground potential. The voltage V_1 across the electrodes is equal to the product of the current *I* (conduction and displacement) and the total complex impedance Z of the cell suspension. The voltage V_2 is equal to the product of I and the resistance R_2 . Thus, the transfer function is directly related to the cell suspension impedance through: $V_2/V_1 = R_2/Z$. The purpose of R_1 is to provide an upper limit on the current I as the impedance Z becomes small at high frequencies, while the unity gain amplifier A_1 acts as a buffer.

Nonlinear response is probed by measuring induced higher harmonics using a four-electrode probe suspended in the cell suspension, as shown in Figure 3. A sinusoidal voltage is applied to the outer electrodes and the cell response across the inner pair of electrodes is measured as a function of frequency, showing plots of the induced harmonics, using the SR780 signal analyzer. Nonlinear dielectric spectroscopy is an extremely sensitive technique, in which the spectra are influenced by the type of organism, its metabolic state, and changes in the conformational states of proteins.

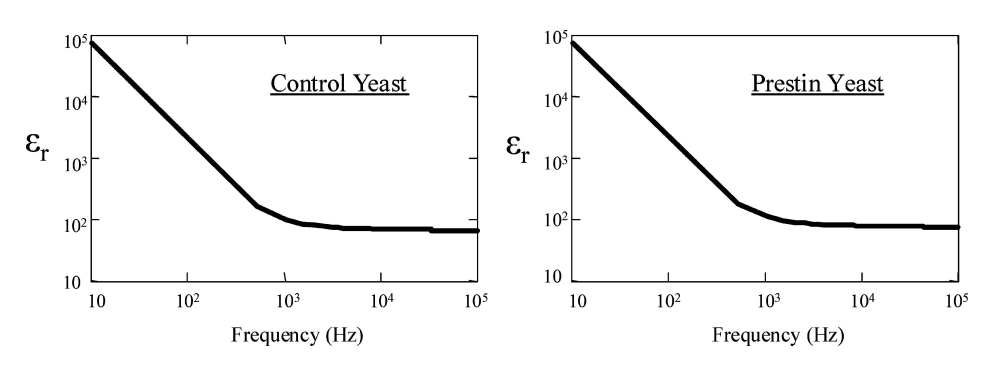


Figure 4. Real part of the relative dielectric constant versus frequency on a log-log scale for two suspensions of yeast (control & prestin-expressed, 10⁸ cells/ml) in deionized water.

Results and Discussion

LINEAR DIELECTRIC RESPONSE

Figure 4 shows plots, on a log-log scale, of the real part of the relative dielectric constant versus frequency for the two suspensions of prestin-GST yeast (*S. cerevisiae*) and GST-expressing yeast of identical concentrations (10⁸ cells/ml) in deionized water

Although it is difficult to discern any difference between the above plots on a logarithmic scale, one can 'zoom in' on the differences by normalizing the data and subtracting the two sets of data. The procedure we used was to plot the parameter Δ , defined in Equation (2) below, versus frequency on a linear-log scale. Here $\varepsilon_p(f)$ represents the relative dielectric constant of the prestin yeast suspension, while $\varepsilon_c(f)$ represents that of the control yeast suspension:

$$\Delta(f) = \frac{\varepsilon_p(f)}{\varepsilon_p(f_0)} - \frac{\varepsilon_c(f)}{\varepsilon_c(f_0)},\tag{2}$$

where f_0 is an arbitrary fixed frequency. This normalization enables one to compensate for any differences that might result from slight changes in cell concentration, electrode spacing, etc. Figure 5 shows a plot of Δ versus f for the case when $f_0 = 10$ kHz, which is near the frequency range of interest, where amplification in mammalian hearing is most significant. Note that there is a rather pronounced hump, which peaks around 25 kHz.

The data in Figure 5 are especially interesting, because they correlates with observations of piezoelectric resonances in outer hair cells that have been isolated from the cochlea [22]. In particular, measurements of the ac admittance versus frequency of an OHC show a peak at around 10 kHz. The peak observed in Figure 5 is at a somewhat higher frequency (\sim 25 kHz) than the reported piezoelectric resonance, and is substantially broader. A plausible explanation is that, in the budding yeast studied here, we have found the prestin to be mainly localized in the endosomes.

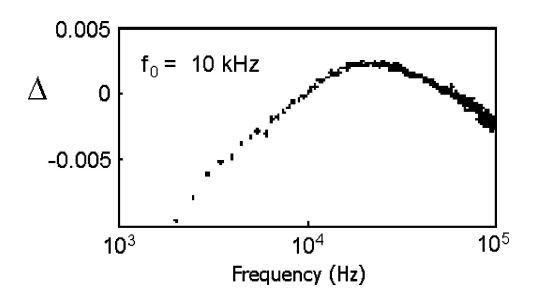


Figure 5. Data designed to highlight differences between the two suspensions, showing Δ (defined in Equation (2), taking $f_0 = 10$ kHz) plotted versus frequency on a linear-log scale.

Since the endosomes are, on average, smaller than OHCs and, in addition, there is a distribution of endosome sizes, one would expect a broad distribution of resonant frequencies whose average value (which scales inversely with the wavelength of sound) would be shifted to a higher frequency.

NONLINEAR DIELECTRIC RESPONSE

The observed nonlinear harmonics also exhibit substantial differences between the two specimens, with somewhat more complex behavior than the linear dielectric response, as shown in Figures 6 and 7. Note that the peak in Figure 6 occurs at a frequency comparable to that observed for the linear response. The amplitude dependence, shown in Figure 7, is also of interest because it may correlate with the membrane potential-dependence of the nonlinear capacitance, which typically shows a peak for membrane potentials of around -50 mV. However, modeling studies will be needed to better correlate the total amplitude in Figure 6 with induced potential differences in specific regions containing prestin.

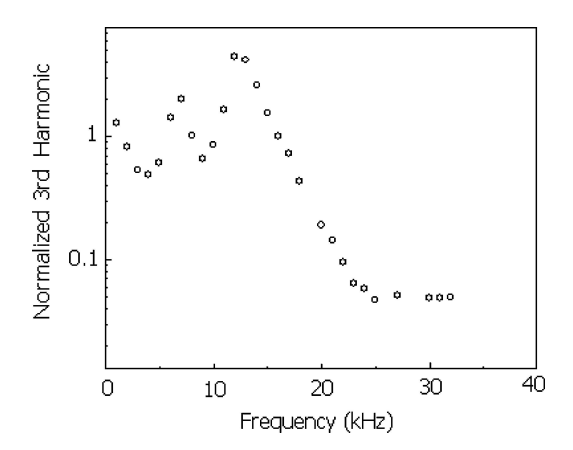


Figure 6. Magnitude of the induced 3rd harmonic response (normalized to 1 mV, where the applied fundamental amplitude is 1 V) as a function of applied fundamental frequency for the suspension of yeast expressing prestin.

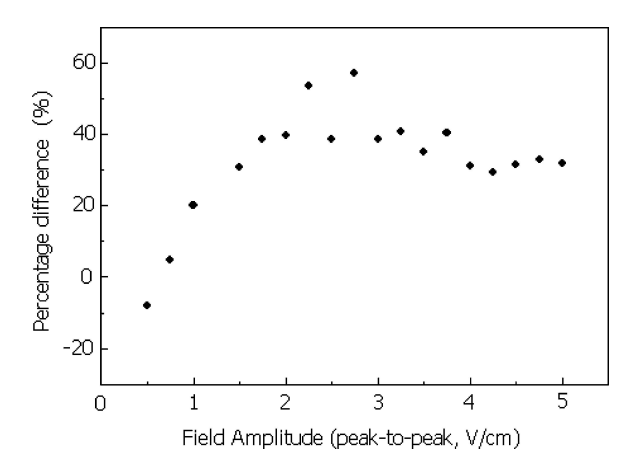


Figure 7. Comparison between the induced third harmonic response of the prestin-expressing yeast suspension and the control specimen expressing only GST, for an applied fundamental frequency of 10 kHz. The data shows percentage difference (prestin versus control) as a function of fundamental voltage amplitude applied across the outer electrodes, spaced 1-cm apart.

Conclusion

Our results suggest that dielectric probes can be used to study the electrical properties of prestin and other proteins, either expressed in live cells or (from our other recent studies on tubulin) as pure protein suspensions. The data obtained for prestin in yeast appears to correlate with other measurements obtained directly on OHCs. Future planned studies include: (1) to further develop the method, through measurements of a large sample base, as a rapid, noninvasive assay; (2) to carry out modeling studies that will enable correlation of the measured data with microscopic properties; and (3) to develop microscopic dielectric probes that can be used in conjunction with imaging (e.g. fluorescence, phase-contrast, etc.) studies.

Acknowledgments

This work was supported, in part, by the Texas Center for Superconductivity and Advanced materials, The Robert A. Welch Foundation (E-1221), the Institute for Space Systems Operations, and by research grant DC 00354 from NIH – NIDCD. The authors would like to thank Y. Kim, Haiying Liu, and Feng Lin for assistance with sample preparation, and J. Wosik, J. Claycomb, and H. Sanabria for helpful discussions and suggestions.

References

 Schwan, H.P.: Electrical Properties of Tissue and Cell Suspensions, in J.A. Lawrence and C.A. Tobias (eds.), *Advances in Biological and Medical Physics*, Vol. V, New York, Academic Press, 1957, pp. 147–209.

- Asami, K., Hanai, T. and Koizumi, N.: Dielectric Properties of Yeast Cells: Effect of Some Ionic Detergents on the Plasma Membranes, *Journal of Membrane Biology* 34 (1977), 145–156.
- For a recent review see Asami, K.: Characterization of Biological Cells by Dielectric Spectroscopy, J. Non-Crystalline Solids 305 (2002), 268–277.
- 4. Prodan, C. and Prodan, E.: The Dielectric Behaviour of Living Cell Suspensions, *J. Phys. D: Applied Phys.* **32** (1999), 335–343.
- Prodan, C.: Dielectric Properties of Live Cell Suspensions, Ph.D. Dissertation, University of Houston (2003).
- Prodan, C., Claycomb, J.R., Prodan, E. and Miller, J.H., Jr.: High-T_c SQUID-Based Impedance Spectroscopy of Living Cells Suspensions, *Physica C* 341–348 (2000), 2693–2694.
- 7. Prodan, C., Mayo, F., Claycomb, J.R., Miller, J.H., Jr. and Benedik, M.J.: Low-Frequency, Low-Field Dielectric Spectroscopy of Living Cell Suspensions, *J. Appl. Phys.* **95** (2004), 3754–3756.
- 8. Woodward, A.M. and Kell, D.B.: On the Nonlinear Dielectric Properties of Biological Systems. *Saccharomyces cerevisiae*, *Bioelectrochem*. & *Bioenerg*. **24** (1990), 83–100.
- 9. Woodward, A.M. and Kell, D.B.: Dual-Frequency Excitation: A Novel Method for Probing the Nonlinear Dielectric Properties of Biological Systems, and its Application to Suspensions of *S. cerevisiae*, *Bioelectrochem. & Bioenerg.* **25** (1991), 395–413.
- 10. Jonscher, A.K.: The 'Universal' Dielectric Response, Nature 267 (1977), 673-679.
- Raicu, V.: Dielectric Dispersion of Biological Matter: Model Combining Debye-Type and 'Universal' Responses, *Phys. Rev. E* 60 (1999), 4677–4680.
- 12. Raicu, V., Sato, T. and Raicu, G.: Non-Debye Dielectric Relaxation in Biological Structures Arises From Their Fractal Nature, *Phy. Rev. E* **64** (2001), 021916-1–10.
- Brownell, W.E., Bader, C.R., Bertrand, D. and De Ribaupierre, Y.: Evoked Mechanical Responses of Isolated Cochlear Outer Hair Cells, Science 227 (1985), 194–196.
- Kachar, B., Brownell, W.E., Altschuler, R. and Fox, J.: Electrokinetic Shape Changes of Cochlear Outer Hair Cells, *Nature* 322 (1986), 365–368.
- Hudspeth, A.J. and Corey, D.P.: Sensitivity, Polarity, and Conductance Change in the Response of Vertebrate Hair Cells to Controlled Mechanical Stimuli, *Proc. Nat. Acad. Sci. USA* 74 (1977), 2407–2411.
- Brownell, W.E., Spector, A.A., Raphael, R.M. and Popel, A.S.: Micro- and nanomechanics of the Cochlear Outer Hair Cells, *Annu. Rev. Biomed. Eng.* 3 (2001), 169–194.
- Zheng, J., Shen, W., He, D.Z.Z., Long, K., Madison, L.D. and Dallos, P.: Prestin is the Motor Protein of Cochlear Outer Hair Cells, *Nature* 405 (2000), 149–155.
- 18. Dallos, P. and Fakler, B.: Prestin, a New Type of Motor Protein, *Nature Rev.: Mol. Cell Biol.* **3** (2002), 104–111.
- Oliver, D., He, D.Z.Z., Klöcker, N., Ludwig, J., Schulte, U., Waldegger, S., Ruppersberg, J.P., Dallos, P. and Fakler, B.: Intracellular Anions as the Voltage-Sensor of Prestin, the Outer Hair Cell Motor Protein, *Science* 292 (2001), 2340–2343.
- Ashmore, J.F.: Forward and Reverse Transduction in Guinea-pig Outer Hair Cells: The Cellular Basis of the Cochlear Amplifier, *Neurosci. Res.* Suppl. 12 (1990), S39–S50.
- Santos-Sachhi, J.: Reversible Inhibition of Voltage-Dependent Outer Hair Cell Motility and Capacitance, J. Neurosci. 11 (1991), 3096–3110.
- Rabbitt, R.D., Ayliffe, H.E., Christensen, D., Pamarthy, K., Durney, C., Clifford, S. and Brownell, W.E.: Evidence of Piezoelectric Resonance in Isolated Outer Hair Cells, *Biophys. J.* 88 (2005), 2257–2265.